Stochastic Kinetic Analysis of the *Escherichia coli* Stress Circuit Using σ^{32}-Targeted Antisense

R. Srivastava,[1,2]* M. S. Peterson,[3] W. E. Bentley[1,2]

[1]Department of Chemical Engineering, University of Maryland, College Park, Maryland 20742, telephone: 301-405-4321; fax: 301-314-9075; e-mail: bentley@eng.umd.ed
[2]Center for Agricultural Biotechnology, University of Maryland Biotechnology Institute, College Park, Maryland, USA
[3]Signal Pharmaceuticals, San Diego, California, USA

Received 28 May 2000; accepted 30 April 2001

Abstract: A stochastic Petri net model was developed for simulating the σ^{32} stress circuit in *E. coli.* Transcription factor σ^{32} is the principal regulator of the response of *E. coli* to heat shock. Stochastic Petri net (SPN) models are well suited for kinetics characterization of fluxes in biochemical pathways. Notably, there exists a one-to-one mapping of model tokens and places to molecules of particular species. Our model was validated against experiments in which ethanol (inducer of heat shock response) and σ^{32}-targeted antisense (downward regulator) were used to perturb the σ^{32} regulatory pathway. The model was also extended to simulate the effects of recombinant protein production. Results show that the stress response depends heavily on the partitioning of σ^{32} within the cell; that is, σ^{32} becomes immediately available to mediate a stress response because it exists primarily in a sequestered, inactive form, complexed with chaperones DnaK, DnaJ, and GrpE. Recombinant proteins, however, also compete for chaperone proteins, particularly when folded improperly. Our simulations indicate that when the expression of recombinant protein has a low requirement for DnaK, DnaJ, and GrpE, the overall σ^{32} levels may drop, but the level of heat shock proteins will increase. Conversely, when the overexpressed recombinant protein has a strong requirement for the chaperones, a severe response is predicted. Interestingly, both cases were observed experimentally.
 Biotechnol Bioeng **75**: 120–129, 2001.
Keywords: stochastic Petri net; σ^{32} stress responses

INTRODUCTION

The induction of cell stress responses, including the σ^{32}-mediated heat shock response (Goff and Goldberg, 1985) and the stringent stress response (Andersson et al., 1996; Harcum and Bentley, 1993), have been shown subsequent to the overexpression of heterologous proteins. Whereas the σ^{32}-mediated stress response in *Escherichia coli* has been well studied, many of the details regarding the regulatory pathways of the σ^{32} protein have yet to be elucidated (Blaszczak et al., 1995; Gamer et al., 1992, 1996; Georgopoulos et al., 1994; Herman et al., 1995; Jubete et al., 1996; Muffler et al., 1997; Nagai et al., 1991; Neidhardt et al., 1996; Neidhardt and VanBogelen, 1981; Strauss, et al., 1987, 1989; Strauss et al., 1990; Tatsuta et al., 1998; Tilly et al., 1989; Tomoyasu et al., 1998; Yura et al., 1993). In particular, the dynamic response of σ^{32} and σ^{32}-mediated proteins to the induction of recombinant proteins remains relatively obscure. σ^{32} is an unstable sigma factor with a half-life on the order of 1 min (Strauss et al., 1987), and is typically present at a basal level of a few molecules in wild-type *E. coli* (Lesley et al., 1987). It is responsible for the production of many chaperone proteins and proteases necessary for the regulation of cell physiology (Georgopoulos et al., 1990, 1994; Gottesman, 1989; Gottesman and Maurizi, 1992; Hendrick and Hartl, 1993; Kitagawa et al., 1991; Parsell and Lindquist, 1993; Yura et al., 1993). A complex of σ^{32} and RNA polymerase, referred to as a σ^{32} holoenzyme ($E\sigma^{32}$), recognizes the genes of these chaperones and proteases. Correspondingly, it binds to the promoter/operator regions and transcribes mRNA. Under normal growth conditions, σ^{32} is outcompeted by another sigma factor, σ^{70}, resulting in comparatively low levels of σ^{32}-mediated regulation. Under heat shock, the cellular concentration of these chaperones and proteases increases; these proteins have been collectively referred to as heat shock proteins (Neidhardt et al., 1996; Strauss et al., 1987, 1989).

A variety of different stresses, such as heat shock, chemical shock (ethanol, phenol, heavy metals, etc.), and overexpression of recombinant protein, trigger the σ^{32}-mediated stress response, resulting in an increase in heat shock proteins (hsps). Although many of the same proteins respond to stress, each individual stress does not induce the identical set, suggesting overlap but distinct regulatory pathways. Under heat shock or ethanol shock, for example, both synthesis and stability of σ^{32} are increased (Neidhardt et al.,

Correspondence to: W. E. Bentley, University of Maryland, 5115 Plant Sciences Building, #36, College Park, MD 20742.
* *Current address:* Department of Chemical Engineering, University of Wisconsin, Madison, WI, USA
Contract grant sponsor: National Science Foundation (GOALI program)

1996). The half-life of σ^{32} may increase by as much as tenfold. The effect on synthesis and/or stability during expression of recombinant proteins has received less attention, although the stability of σ^{32} was shown to be increased upon induction of human prourokinase (Kanemori et al., 1994).

In this article we develop a stochastic model to probe the σ^{32} regulatory pathway. Using a plasmid vector that synthesizes σ^{32}-targeted antisense mRNA, we previously perturbed the σ^{32} circuit and transiently observed the native and antisense-modulated responses (Srivastava et al., 2000). In this work, we compare the experimental results to the predictions of our stochastic model. Also, we incorporate a generic recombinant protein production pathway to simulate stress due to the expression of recombinant protein. Results indicate the partitioning of σ^{32} significantly influences the response. Our results also demonstrate both the appropriateness and conceptual simplicity of modeling genetic circuits, such as σ^{32}, using stochastic Petri nets.

BACKGROUND

σ^{32} Metabolism

The σ^{32}-regulated stress proteins, DnaK, DnaJ, and GrpE, in addition to being chaperones for misfolded/aberrant proteins, have been shown to form a complex that binds σ^{32} (Gamer et al., 1992, 1996; Strauss et al., 1989). When bound to this complex, σ^{32} is presented to FtsH, another σ^{32}-regulated stress protein, for degradation (Gamer et al., 1996; Herman et al., 1995; Tomoyasu et al., 1995). This degradation pathway is depicted in Figure 1. Although the exact sequence of events in the formation of the chaperone–σ^{32} complex is unknown, based on in vitro studies it is believed that the DnaJ–σ^{32} binding step is rate limiting (Gamer et al., 1996). The result of these interactions is a feedback control mechanism for maintaining the physiologically appropriate level of σ^{32}.

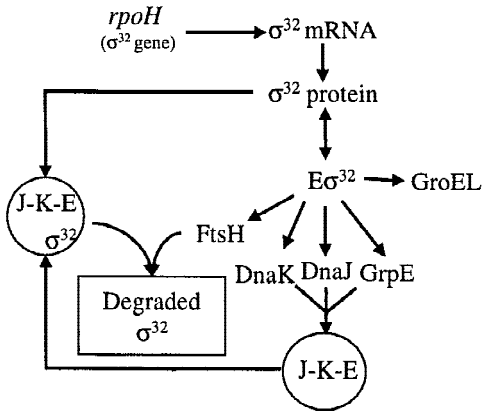

Figure 1. σ^{32} Regulatory pathway. After the σ^{32} factor is synthesized, it helps catalyze the synthesis of a number of other proteases and chaperone proteins, collectively referred to as heat shock proteins (hsps). Shown is a small sample of hsps and how they participate in the σ^{32} degradation process.

As noted earlier, the synthesis and/or accumulation of σ^{32} increases under heat shock and other stresses, including the production of recombinant human interleukin-2 (hIL-2) (DeLisa et al., 2000; Strauss et al., 1990). Also, under many stress conditions, abnormal/misfolded proteins are formed (Neidhardt et al., 1996). These misfolded proteins are believed to compete for the same chaperones that are required for the degradation of σ^{32}. Consequently, the combination of these mechanisms contributes to an observed tenfold increase in the half-life of σ^{32} under stress (Kanemori et al., 1994; Strauss et al., 1987) and its subsequent accumulation. The increased concentration of σ^{32} allows it to better compete with other σ-factors for the available RNA polymerases.

Model Development

Ordinary differential equations are often used to quantitatively describe biochemical systems at the cellular and molecular levels. Such descriptions are valid when the amount of the reacting species is large and fluctuations of individual reactants do not contribute to the overall system behavior. However, when describing small quantities of reactants, fluctuations can potentially play a significant role in determining how reactions proceed. Regulatory molecules, including sigma factors, are generally present at low levels. How such molecules are regulated, as well as how they carry out their regulatory duties, in the face of stochastic fluctuations, is not trivial. Modeling the molecular behavior deterministically can be grossly misleading, especially if a kinetic trajectory lies close to a stable or unstable node for the system. Fluctuations can lead to results not predicted deterministically (Érdi and Tóth, 1988).

Because there are relatively few σ^{32} molecules per cell, a stochastic model, rather than a deterministic model, was used for quantitative description of the σ^{32} regulatory pathway. Stochastic models are better suited for quantitative description of events in which a small number of discrete entities are interacting (Arkin et al., 1998; Érdi and Tóth, 1988; Kurtz, 1972; McAdams and Arkin, 1997, 1998, 1999). Specifically, a stochastic Petri net (SPN) modeling formalism was employed. Petri nets have been used to model biological systems (Chin and Willsky, 1989; Goss and Peccoud, 1998, 1999; Ouchi and Tazaki, 1998; Reddy et al., 1993). SPNs are effective for modeling event-driven processes for continuous-time, discrete-space, distributed systems (Marsan et al., 1995). They are also isomorphic to hidden Markov chains. Because chemical reactions are inherently Markov jump processes, they are effectively modeled with SPNs.

An SPN is made up of *places*, *tokens*, and *transitions.* Places, denoted by large open circles in Figure 2, represent the chemical species involved in a reaction. A place can hold tokens, where the number of tokens represents the quantity of the given chemical species. For the reaction shown (Fig. 2), if each token represents a molecule, there exists two molecules of reactant A, three molecules of re-

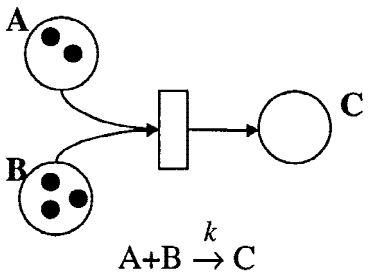

Figure 2. Sample stochastic Petri net (SPN). The depicted SPN shows the reaction $A + B \rightarrow C$, with a deterministic reaction rate constant of k. The large circles are *places* and represent the given chemical species. The number of *tokens*, shown by the smaller opaque circles within the places, are proportional to amount of chemical species present. The *transition*, depicted by the rectangle, represents the given chemical reaction. A reaction is described by the direction of the arrows or *arcs* between the places and the transition.

actant B, and zero molecules of product C. The transition, denoted by a rectangle, represents a chemical reaction. Chemical species that are consumed in a reaction have an arrow or an *arc* pointing from their place to the transition. Reaction products have an arc pointing from the transition to their place. The reaction depicted in Figure 2 is a single, irreversible reaction. Because there is only one transition present, whenever such a reaction occurs, the stoichiometric number of reactant tokens used is destroyed and the stoichiometric number of product tokens is created in the product place.

The occurrence of any given reaction is determined by a weighted negative exponential probability density function, and the weighting of the function is based on the deterministic rate parameter and the number of tokens (amount of chemical species) available for the reaction. For a first order reaction of the form:

$$A \xrightarrow{k} B$$

where k is the deterministic rate constant, and the stochastic rate constant, β, and k are equal. For a reaction of the form:

$$A + B \xrightarrow{k} C$$

the stochastic rate constant is:

$$\beta = \frac{k}{V N_A}$$

where V is the cell volume and N_A is Avogadro's number (Gillespie, 1976; Goss and Peccoud, 1998; McAdams and Arkin, 1998).

If more than one potential reaction can occur, the time at which each reaction will occur is determined randomly from the probability density function. The earliest reaction is allowed to occur, and the number of tokens in all places is appropriately updated. Because the tokens have then shifted to new places, the weighting of the density functions is recalculated. The time at which each possible reaction can occur is again randomly distributed, and the process is repeated. The simulation is terminated when a predetermined criterion is met, such as the passage of certain time period. It should be noted that this type of implementation of SPNs is equivalent to the First Reaction Method of the Gillespie algorithm (Gillespie, 1976).A stochastic Petri net based on the synthesis/degradation regulatory pathway of σ^{32} was constructed as shown in Figure 3. Because σ^{32} synthesis is of explicit concern, places for the σ^{32} gene, mRNA, and protein were each included. To determine the impact of σ^{32}-targeted antisense mRNA on the synthesis of σ^{32}-related proteins, a simplified form of the GroEL pathway was included. In this way, GroEL, a σ^{32}-mediated stress response protein, can serve as an indicator of σ^{32}-mediated transcription. That is, because GroEL has not been shown to impact the σ^{32} life cycle (Gamer et al., 1996), it can serve indirectly as an indicator of σ^{32}-regulated transcription and the stress response. Another model simplification was made for the chaperones DnaK, DnaJ, and GrpE. In particular, because the DnaJ–σ^{32}-binding step is rate limiting for complex formation (Gamer et al., 1996), one place for the chaperone complex was defined and is referred to as the J-complex. This J-complex is therefore a lumped constituent of the actual system. Likewise, there are lumped reaction rates (e.g., GroEL protein formation directly from *groEL* gene transcription), when appropriate, which enable simplification.

Model Implementation

Parameter values used are listed in Table I. It was assumed that a 1 n*M* concentration of any given species was equal to one molecule of that species (Arkin et al., 1998). One token was set as equivalent to one molecule of any given chemical species. To simulate the effect of σ^{32}-targeted antisense synthesis (Srivastava et al., 2000), the translation rate of σ^{32} was simply decreased. This presumes that σ^{32}-antisense hybridizes with its complementary mRNA, preventing ribosomal translation of the mRNA (Daugherty et al., 1989; Good and Nielsen, 1998; Murray, 1992). The antisense/mRNA duplex is degraded by RNases that degrade either: (1) nonhybridized single-stranded mRNA; or (2) a double-stranded portion of the duplex (Belasco and Brawerman, 1993). Because the stochastic model is based on the probability of a reaction occurring, and because the antisense decreases the probability of translation occurring, the antisense-mediated downregulation was simulated by a reduced translation rate. In this case it was necessary to utilize this simplified approach for simulating antisense downregulation, because the in vivo binding kinetics of the σ^{32} antisense RNA, as well as the synthesis and degradation kinetics, are as yet unavailable.

For simulating the effects of recombinant protein produc-

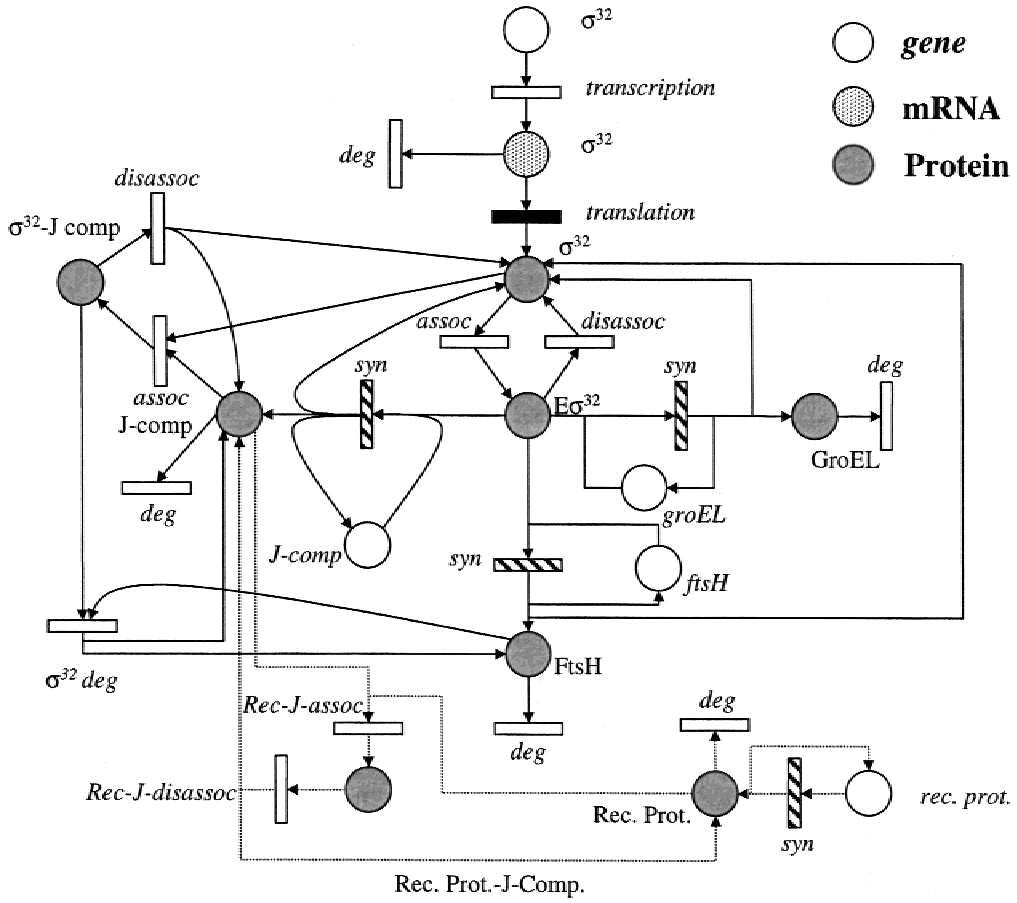

Figure 3. SPN of the σ^{32} genetic regulatory circuit. All simulations were based on the SPN shown. The arcs made up of dotted lines were included only for the recombinant protein simulations.

tion, the generic binding constant between the recombinant protein and the J-complex was varied. In this way, predictions of a σ^{32}-mediated stress response could be generated. Three scenarios were evaluated: low requirement for chaperone mediation, equal requirement, and strong requirement for chaperone mediation, with their corresponding values shown in Table II. Although the model of the σ^{32} circuit was in part lumped, we assumed that it could be modeled as a Markov process, allowing SPN implementation.

Experimental Conditions and Simulation Details

In our previous work (Srivastava et al., 2000), we demonstrated that IPTG-induced σ^{32} antisense mRNA mediated a decrease in σ^{32} sense mRNA, σ^{32} protein, and GroEL protein. We further demonstrated that, in the presence of σ^{32} antisense, the activity level of a recombinant organophosphorous hydrolase was increased substantially. GroEL was monitored as a marker protein of the σ^{32}-related stress response, as it has little if any direct impact on σ^{32} metabolism. It provides, therefore, a basis for correlation between simulations and our previous data as well as others (Gamer et al., 1992, 1996; Strauss et al., 1987, 1990).

The σ^{32} SPN simulations were run using ULTRASAN, a software package for modeling stochastic activity networks (Sanders, 1995). The ULTRASAN software was kindly provided by Dr. Sanders (Center for Reliable and High-Performance Computing at the University of Illinois at Urbana–Champaign).

The time duration used for simulations was 30 min. Experimentally, we found that antisense reached a maximum within the first 30 min postinduction, and most of the metabolic activity occurred within this timeframe. Also, a 30-min timeframe enables one to safely neglect the effects of cell doubling. Places were seeded with 1 to 15 tokens, and simulations were performed until a steady state was reached. The number of tokens available at steady state was considered the nonstressed state of the cell. These steady-state-level concentrations were subsequently used as the starting point for all further simulations.

RESULTS

Transient Analysis of Ethanol Shock and Comparison to Data

When subjected to ethanol (4% v/v), *E. coli* increased σ^{32} levels by over ten-fold (Srivastava et al., 2000). In simula-

Table I. σ^{32} stress circuit rate constants.

Transition	Deterministic rate constant	Reference
FtsH degradation	7.40×10^{-11} s^{-1}	Herman et al. (1995)[a]
FtsH synthesis	4.41×10^{6} (M s)$^{-1}$	Assumed to be same as J-comp synthesis
GroEL degradation	1.80×10^{-8} s^{-1}	Kanemori et al. (1994)[a]
GroEL synthesis	5.69×10^{6} (M s)$^{-1}$	Kanemori et al. (1994)[a]
J-disassociation	6.40×10^{-10} s^{-1}	Kanemori et al. (1994)[a]
J-production	4.41×10^{6} (M s)$^{-1}$	Kanemori et al. (1994)[a]
Holoenzyme association	0.7 s^{-1}	Blaszczak et al. (1995)[b]
Holoenzyme disassociation	0.13 s^{-1}	Blaszczak et al. (1995)[b]
σ^{32} mRNA decay	1.4×10^{-6} s^{-1}	Adjusted to get 9 molecules σ^{32} under nonstress conditions
σ^{32}–J-association rate	3.27×10^{5} (M s)$^{-1}$	Gamer et al. (1996)
σ^{32} degradation	1.28×10^{3} (M s)$^{-1}$	Tomoyasu et al. (1995)[a]
σ^{32}–J-disassociation rate	4.4×10^{-4} s^{-1}	Gamer et al. (1996)
σ^{32} transcription	1.4×10^{-5} s^{-1}	Adjusted to get 9 molecules σ^{32} under nonstress conditions
σ^{32} translation	0.007 s^{-1}	Adjusted to get 9 molecules σ^{32} under nonstress conditions
Recombinant protein–J-association	Refer to Table I	Estimated based on Kanemori et al. (1994)
Recombinant protein–J-disassociation	4.40×10^{-5} s^{-1}	Estimated based on Kanemori et al. (1994)
Recombinant protein synthesis	4.00 s^{-1}	Estimated based on Kanemori et al. (1994)
Recombinant protein degradation	9.99×10^{-5} s^{-1}	Estimated based on Kanemori et al. (1994)

[a]Derived from data.
[b]Fitted to data.

tions, the transcription rate constant for σ^{32} mRNA was increased by two orders of magnitude and there was no change in the concentration of any of the downstream species (data not shown). However, increasing the stochastic kinetic translation rate constant of σ^{32} by as little as 10% resulted in substantial increases in all σ^{32}-mediated stress response proteins. Hence, to simulate the effect of ethanol on σ^{32}, the translation rate constant was increased. Specifically, increasing the translation rate constant from the normal growth value, 0.007, to 0.15, resulted in a simulated response that matched our experimental result with a high degree of accuracy (Fig. 4).

Conversely, by raising the translation rate constant from 0.007 to 0.02, antisense-mediated downregulation of the ethanol stress was simulated; that is, after ethanol stress, but without antisense production, σ^{32} rose within 3 min to a level 12-fold higher than at preinduction. After the first 3 min, σ^{32} decreased continuously to a level ten-fold higher than the preinduction level. However, when σ^{32} antisense was induced simultaneously with ethanol stress, the σ^{32} levels rose only 2.5-fold over the preinduction value. This was reached within 6 min and the σ^{32} level was steady for another ~12 min, after which it gradually declined to 2.4-Fold the preinduction level.

Table II. Recombinant protein–J-complex association rate constants.

Chaperone requirement	Rate constant
Low	1.42×10^{3} (M s)$^{-1}$
Equal	3.27×10^{5} (M s)$^{-1}$
High	7.11×10^{5} (M s)$^{-1}$

In Figure 4B, the results for σ^{32}-regulated GroEL are shown. Again, in both cases, the simulation and experiment were in agreement. GroEL increased further in the case of ethanol stress without σ^{32} antisense. It is also noteworthy that only the translation rate constant of σ^{32} was changed and the effects on both σ^{32} and GroEL were predicted.

It is important to highlight that this stochastic simulation allows generation of variance data for any given biochemical species. Hence, it is possible to determine a predicted distribution of the molecule within the cell population. In Figure 4, mean ± standard deviation data are depicted. Interestingly, throughout the ethanol stress experiment, σ^{32} was predicted to be widely distributed among the cell population. For the antisense production case, the variance was much smaller, suggesting a much closer clustering of cellular σ^{32} to the mean level. At present there are no data

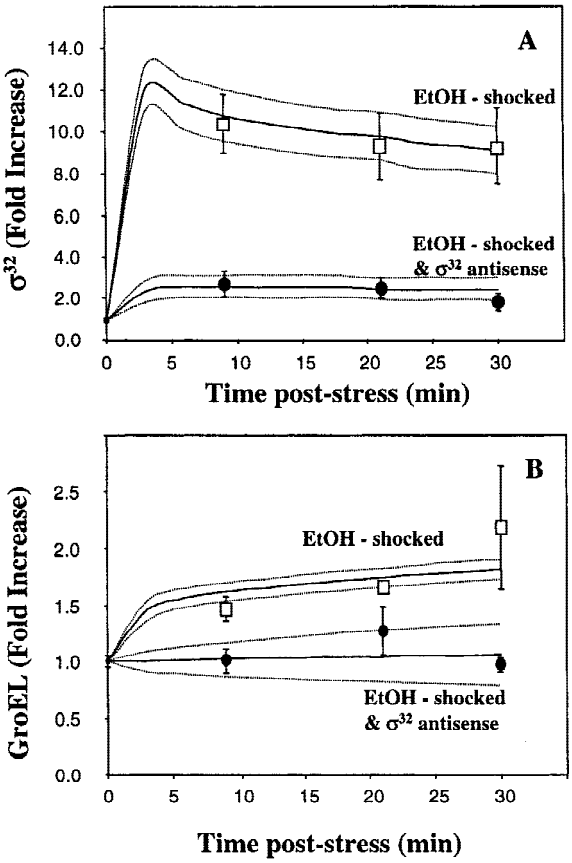

Figure 4. Ethanol stress response dynamics with and without antisense. (A) σ^{32} simulation results (thick solid line) ± standard deviation (thin dotted lines) compared with experimental data (points with error bars). (B) GroEL simulation results (thick solid line) ± standard deviation (thin dotted lines) compared with experimental data (points with error bars). In all simulations there were 9 tokens of σ^{32} and 217 tokens of GroEL initially.

available for confirmation of this prediction. The importance of distribution data is discussed later. In summary, the model proved to be remarkably accurate via comparison to available transient data. For the situation in which *E. coli* was stressed, but with no σ^{32} antisense, a transient peak was both predicted and found experimentally (Srivastava et al., 2000; Strauss et al., 1987).

Predicted σ^{32} Distribution

The σ^{32} regulatory pathway (depicted in Fig. 2) was simplified in this work by distinguishing three distinct pools; that is, σ^{32} exists either as a freely suspended protein, as a complex with RNA polymerase, or as a complex with heat shock proteins DnaK, DnaJ, and GrpE. Under nonstress and stress conditions, the vast majority of the σ^{32} (>99%) was predicted to be complexed to the heat shock proteins, and only a very small amount was free or in the form of the holoenzyme (not shown). Consequently, the σ^{32}–J-complex pool provides a potential reservoir of σ^{32} that can be readily tapped for gene transcription without a corresponding increase in σ^{32} synthesis. In this way, DnaK, GrpE, and DnaJ can act in a buffering capacity so that the concentration of σ^{32} available for transcription of stress-related genes is not dependent solely on the synthesis and degradation pathways. Also, because our model predicts that only a small amount of σ^{32} is complexed with the RNA polymerase, it is further suggested that only a very small amount of Eσ^{32} is needed to effect the σ^{32}-mediated stress response. Thus, under a stress response, once σ^{32} synthesis is increased the ability to complex σ^{32} with chaperones becomes saturated and the remaining free σ^{32} is available to form σ^{32}-holoenzymes. Even a slight increase in free σ^{32}-holoenzyme results in rapid production of σ^{32}-mediated stress proteins, resulting in increased σ^{32} buffering capacity, which, in turn, increases the capacity for σ^{32} degradation. The principal result, therefore, is a rapid increase in σ^{32} followed by a rapid poststress decrease. This underscores the agreement with the role of σ^{32} as a rapid initiator of the heat shock response. The metabolic direction of the cell is altered within minutes, which would otherwise be difficult to accomplish based on synthesis and degradation of σ^{32} alone.

Stress Response to Overexpression of Recombinant Proteins

The effect of recombinant protein expression on this circuit was simulated in two ways. The first method, which directly interrupts the distribution of σ^{32} was effected by altering the requirement of the recombinant protein for the J-complex. This complex is the most effective and most active of the five chaperone systems for mediating protein aggregation under stress (Mogk et al., 1999). Correspondingly, it is reasonable to simulate the sequestration of the chaperone complex away from its natural functions to the modulation of recombinant proteins by lowering the associated "affinity" binding constant. A substantial impact on the dynamics of σ^{32} was found (Fig. 5). In cases where there is a strong requirement, a twofold transient peak was observed within 10 min. When σ^{32} antisense was simultaneously induced, a similar trajectory was predicted, but only after a slight delay, due to the attenuation of σ^{32} synthesis. Figure 6 shows that the vast majority of σ^{32} was in the free form, regardless of whether antisense was produced. In both cases, after the first 6 min, there was no σ^{32} associated with the J-complex. Thus, the stabilization of σ^{32} was predicted, potentially leading to a σ^{32}-mediated stress response. Also, simulations suggest that a steady state in the distribution of σ^{32} was reached within 10 min. The distribution dynamics of the equal "affinity" case were similar, except that the σ^{32} trajectories increased to a steady-state level monotonically (data not shown).

When the requirement of the recombinant protein for the J-complex was lower than that of σ^{32}, a much different response was predicted. Notably, the overall level of σ^{32} decreased (Fig. 5), and the decrease was more rapid in the presence of σ^{32} antisense mRNA. Once again, this was probably due to the lack of new σ^{32} translation. Simulation results for the low requirement case are depicted in Figure

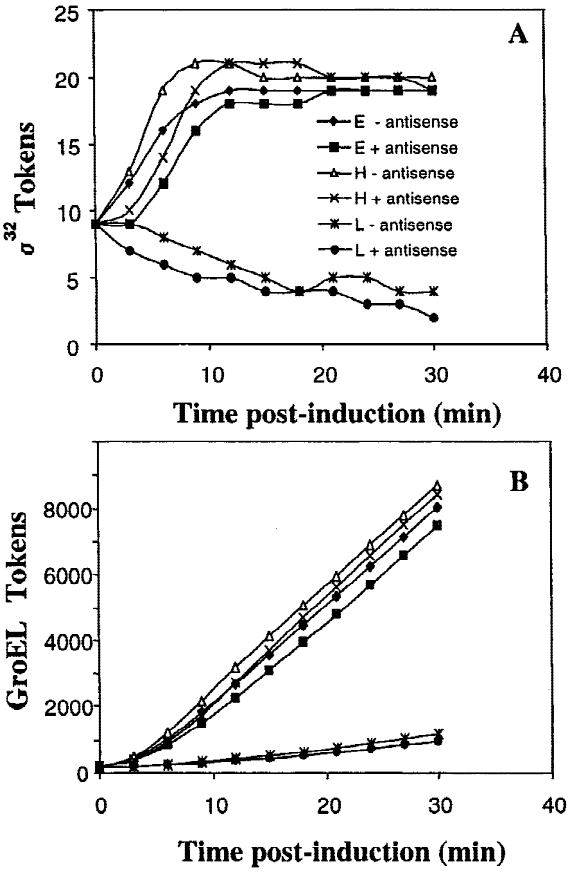

Figure 5. Dynamics for (A) σ^{32} and (B) GroEL following induction of recombinant protein with varying affinity for DnaK, DnaJ, and GrpE. H denotes that the recombinant protein has a stronger or "higher" requirement for the J-complex than σ^{32}, whereas, for L, the situation is reversed. For E, σ^{32} and the recombinant protein require equally the J-complex for folding.

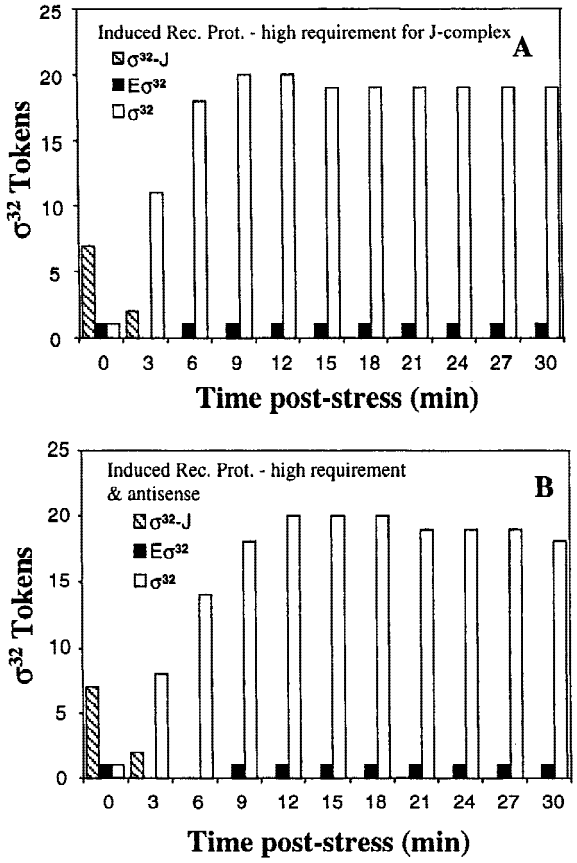

Figure 6. Partitioning of σ^{32} during recombinant protein expression in the case of strong J-complex requirement. The pools into which σ^{32} were partitioned were free σ^{32} (s32), complexed to RNA polymerase (Es32), or complexed with DnaK, DnaJ, and GrpE (s32-J). (A) Without antisense production. (B) With antisense production. Initially, there were seven tokens of σ^{32}–J, one token of Eσ^{32}, and one token of free σ^{32}.

7. In the induced case without antisense, an initial increase in J-complex-associated σ^{32} was found. Interestingly, an increase in free σ^{32} was also found, but was only twofold over a 12 to 15-min period. In the induced/antisense case, no initial increase in J-complex-associated s^{32} was found; however, after 3 min the predictions were similar to the case without antisense. Hence, in both cases, a σ^{32}-mediated stress response could result, which was substantiated by a gradual increase in GroEL (Fig. 5B). The predicted response was effected in this case by the increase in free σ^{32}, which could bind to the holoenzyme. The holoenzyme level was predicted to drop to zero, which indicates that each holoenzyme is active for a short time, disassembled, and then the σ^{32} rapidly reassigned.

Although little is known regarding the in vivo levels of DnaK and GroEL after the induction of recombinant proteins, substantial data exist regarding levels after heat shock, which is similar to ethanol addition (Ellis and Hart, 2000; Houry et al., 1999; Mogk et al., 1999). Both DnaK and GroEL were observed to increase two- to threefold after heat shock (which is consistent with Srivastava et al. [2000]), after ethanol addition and with current simulations (Fig. 4B). Likewise, as noted earlier, σ^{32} predictions are in close agreement with literature data (Strauss et al., 1990). In the presence of recombinant protein production, few reports have appeared (Gill et al., 2000; Jurgen et al., 2000; Ramirez and Bentley, 1995) that measured the levels of GroEL or DnaK transcription and/or translation after protein induction. After the expression of chloramphenicol acetyltransferase (CAT; Gill et al., 2000; Ramirez and Bentley, 1999), there was no significant change in either GroEL or DnaK transcription or translation within the first 30 min, but a gradual increase in GroEL over 8 postinduction. These results are entirely consistent with the low requirement simulations in Figure 7. Although neither CAT/GroEL nor CAT/DnaK immunoprecipitation experiments were performed, it is conceivable that CAT would have a limited need for these chaperones to fold properly. CAT is an endogenous bacterial protein, very stable and typically active in a variety of cells, and, because of these properties, CAT is widely used as a reporter. Hence, the induction of CAT is likely to result in a rapidly synthesized, properly folded protein. Furthermore, its size (M_r 27 K) is on the low end of the reported in vivo substrates for both GroEL (20 to 60 K; [Houry et al., 1999]) and DnaK (primarily occupied with >90 K proteins under stress [Mogk et al., 1999]).

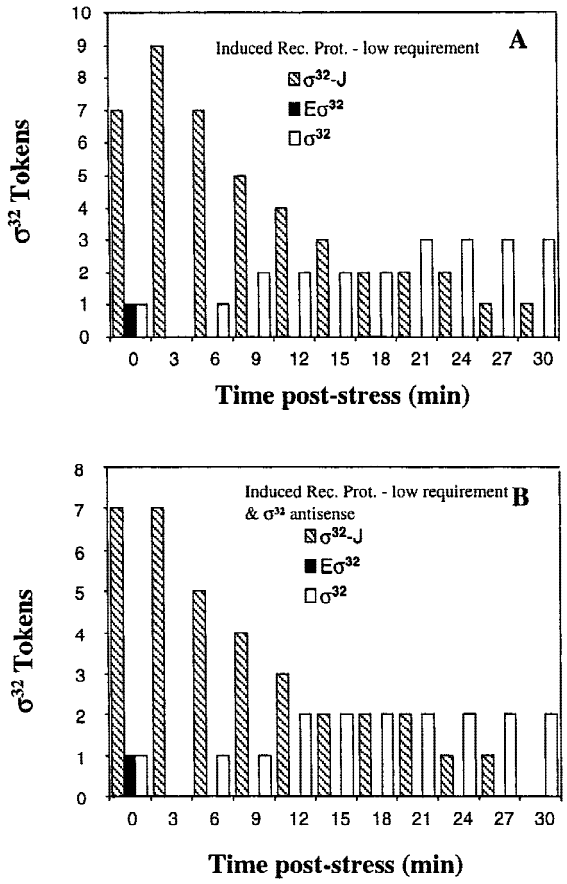

Figure 7. Partitioning of σ^{32} during protein expression in the case of a low requirement for J-complex. The pools into which σ^{32} were partitioned were free σ^{32}, complexed with RNA polymerase ($E\sigma^{32}$), or complexed with DnaK, DnaJ, and GrpE (σ^{32}-J). (A) Without antisense production. (B) With antisense production. Initially, there were seven tokens of σ^{32}–J, one token of $E\sigma^{32}$, and one token of free σ^{32}.

According to Jurgen et al. (2000), α-glucosidase of yeast was overexpressed as insoluble aggregates in *E. coli* RB791. A rapid and dramatic increase in dnaK and ibpB transcription was observed. Importantly, they also found significant quantities of both DnaK and GroEL protein in the insoluble aggregate fraction, suggesting binding of the chaperones to the α-glucosidase. This is confirmatory of our simulations with a high-"affinity" constant, where, upon induction, the recombinant protein sequesters the chaperones, which in turn are less likely to associate with σ^{32}, enabling a rapid increase in holoenzyme and a rapid stress response.

DISCUSSION

The mapping of regulatory pathways in biochemical systems correlates strongly with the Petri net formalism. As such, the Petri net is a natural method for modeling metabolic systems. The Petri net developed here was particularly useful because a change in one rate constant (the σ^{32} translation rate constant) provided simulations that agreed well with experimental results of both σ^{32} and GroEL. With this model, various hypotheses were confirmed and experimental results were validated. Specifically, we proposed that downregulating σ^{32} would result in the secondary downregulation of GroEL. As a consequence, the model also demonstrated that the regulatory pathway and feedback regulation of σ^{32} as indicated was sufficient to account for the transient peak in σ^{32} levels under stress, and under stress attenuated by σ^{32} antisense RNA. Also, it has been hypothesized that the overproduction of recombinant proteins could induce a σ^{32}-mediated stress response (Gill et al., 2000; Goff and Goldberg, 1985; Ramirez and Bentley, 1995). Although the induction of hsps after overexpression of abnormal proteins has been widely reported (e.g., Goff and Goldberg), there have been no kinetic predictions of the specific mechanisms leading to this response. The prevailing hypothesis is the sequestration of chaperones and proteases from normal metabolic functions to the targeting and degradation of foreign recombinant proteins (Baneyx, 1999). The model shown here provides some insight into this process by predicting that key control points in the σ^{32} stress response system are the translation of σ^{32} mRNA and association of the DnaK–DnaJ–GrpE complex with the majority of σ^{32}. In agreement, the increased synthesis of σ^{32} was shown to be primarily translationally regulated (Cha et al., 1999). Also, the ability of DnaK–DnaJ–GrpE to buffer σ^{32} further explains the ability of the cells to regulate tight control of over the σ^{32}-mediated stress response, even though a potentially large variance exists among the population.

One of the major benefits of using a stochastic Petri net over other modeling formalisms was the ease by which it was possible to translate the postulated σ^{32} regulatory pathway directly to the SPN modeling paradigm. An inherent benefit of such a method is that gross errors in the regulatory pathway should quickly be revealed in the simulations. Subsequently, changes made to the proposed pathway are easily incorporated into the SPN. Furthermore, the stochastic nature of the model provides the added benefit of generating variance data. To assume a homogeneous distribution of protein across a cell population can be misleading (Imanaka and Aiba, 1981). It may be that the variance and/or distribution of a particular species may have a critical impact on metabolism (Arkin et al., 1998; McAdams and Arkin, 1998, 1999) and bioreactor performance (Bentley and Quiroga, 1993). Our simulations indicate this was the case for free σ^{32}, wherein the DnaK–DnaJ–GrpE-mediated σ^{32} degradation/"buffering" pathway, as suggested here, might have evolved to provide rapid transients in level signaling the need for response.

The simulation results further suggest that the strength of the σ^{32} response is dependent on a number of factors, including the relative overall abundance of σ^{32} and the distribution of σ^{32} among the three complexes considered. In addition, the relative rate of recombinant protein synthesis was important. In Figure 7, by the end of the simulation, almost no σ^{32} was bound to the J-complex. Yet the stochas-

tic constant for binding of the recombinant protein was much less than that of σ^{32}. However, the probability of a reaction occurring was greater when there was a large number of reactants, in this case recombinant proteins. On a per-molecule basis, σ^{32} was initially more likely to bind with the J-complex (based on the rate constant), yet the abundance of the recombinant protein (approximately 7000 tokens at the end of 30 min) made it far more likely that the J-complex would encounter the recombinant protein.

Another key aspect of the σ^{32}-mediated stress response simulation was the speed by which it was allocated to the various partitions. In the high-affinity scenario, as soon as the chaperone-bound σ^{32} was degraded or disassociated, it was replaced with recombinant protein. σ^{32} was therefore unable to compete with the recombinant protein and was forced into the other two partitions where it quickly accumulated. In the low-affinity case, σ^{32} was better able to compete with the recombinant protein for the J-complex. The result was that the σ^{32} degradation pathway was not entirely shut down, but the strength of the stress response was substantially mitigated. Even in the low-affinity condition, a stress response was predicted based on GroEL levels. Note, however, that the present model does not account for the stress-mediated induction of protein degradation (Ramirez and Bentley, 1999). In this case, although the σ^{32}-mediated response was increased due to protein overexpression and saturation of the chaperones, it is likely that the protein would have been targeted for degradation via Lon, ClpB, or other stress-induced proteases. This, in turn, would have attenuated the overall response. As a result, even though the predictions of GroEL increased within 30 min after CAT expression, we previously observed no change in GroEL until 4 to 8 h postinduction. It might have been the case that, early in the postinduction period, CAT was partially degraded, and this attenuated the stress response until sufficient CAT was synthesized that it saturated the buffering capacity from the J-complex. We did observe CAT degradation products throughout (Ramirez and Bentley, 1995). Such results emphasize the importance of σ^{32} partitioning and provide direction for further experimentation.

The authors thank Dr. R. Burgess for insightful discussions.

References

Andersson L, Yang S, Neubauer P, Enfors SO. 1996. Impact of plasmid presence and induction on cellular responses in fed batch cultures of *Escherichia coli.* J Biotechnol 46:255–263.

Arkin A, Ross J, McAdams HH. 1998. Stochastic kinetic analysis of developmental pathway bifurcation in phage lambda-infected *Escherichia coli* cells. Genetics 149:1633–1648.

Baneyx F. 1999. Recombinant protein expression in *Escherichia coli.* Curr Opin Biotechnol 10:411–421.

Belasco JG, Brawerman G, editors. 1993. Control of messenger RNA stability. San Diego, CA: Academic Press.

Bentley WE, Quiroga OE. 1993. Investigation of subpopulation heterogeneity and plasmid stability in recombinant *Escherichia coli* via a simple segregated model. Biotechnol Bioeng 42:222–234.

Blaszczak A, Zylicz M, Georgopoulos C, Liberek K. 1995. Both ambient temperature and the DnaK chaperone machine modulate the heat shock response in *Escherichia coli* by regulating the switch between σ^{70} and σ^{32} factors assembled with RNA polymerase. EMBO J 14:5085–5093.

Cha HJ, Srivastava R, Vakharia VN, Rao G, Bentley WE. 1999. Green fluorescent protein as a noninvasive stress probe in resting *Escherichia coli* cells. Appl Environ Microbiol 65:409–414.

Chin TM, Willsky AS. 1989. Stochastic Petri net modeling of wave sequences in cardiac arrhythmias. Comput Biomed Res 22:136–159.

Daugherty BL, Hotta K, Kumar C, Ahn YH, Zhu JD, Pestka S. 1989. Antisense RNA: Effect of ribosome binding sites, target location, size, and concentration on the translation of specific mRNA molecules. Gene Anal Tech 6:1–16.

DeLisa MP, Valdes JJ, Bentley WE. Mapping perturbation-induced quorum (AI-2) signaling links stress-mediated transcription circuits in recombinant *Escherichia coli.* J Bacteriol 183:2918–2928.

Ellis RJ, Hart FU. 2000. Folding and binding: Problems with proteins. Curr Opin Struct Biol 10:13–15.

Érdi P, Tóth J. 1988. Mathematical models of chemical reactions: Theory and applications of deterministic and stochastic models. Princeton, NJ: Princeton University Press.

Gamer J, Bujard H, Bukau B. 1992. Physical interaction between heat shock proteins DnaK, DnaJ, and GrpE and the bacterial heat shock transcription factor σ^{32}. Cell 69:833–842.

Gamer J, Multhaup G, Tomoyasu T, McCarty JS, Rudiger S, Schonfeld H, Schirra C, Bujard H, Bukau B. 1996. A cycle of binding and release of the DnaK, DnaJ and GrpE chaperones regulates activity of the *Escherichia coli* heat shock transcription factor σ^{32}. EMBO J 15:607–617.

Georgopoulos CD, Ang D, Liberek K, Zylicz M. 1990. Properties of the *Escherichia coli* heat shock proteins and their roles in bacteriophage growth. In: Motimoto RI, Tissieres A, Georgopoulos C, editors. Stress proteins in biology and medicine. Cold Spring Harbor, NY: Cold Spring Harbor Laboratory Press. p 191–221.

Georgopoulos CD, Liberek K, Zylicz M, Ang D. 1994. Properties of the heat shock proteins of *Escherichia coli* and the autoregulation of the heat shock response. In: Motimoto RI, Tissieres A, Georgopoulos C, editors. The biology of heat shock proteins and molecular chaperones. Cold Spring Harbor, NY: Cold Spring Harbor Laboratory Press. p 209–249.

Gill RT, DeLisa MP, Shiloach M, Holoman TR, Bentley WE. 2000. OmpT expression and activity increase in response to recombinant chloramphenicol acetyltransferase overexpression and heat shock in *E. coli.* J Mol Microbiol Biotechnol 2:283–289.

Gillespie DT. 1976. A general method for numerically simulating the stochastic time evolution of coupled chemical reactions. J Comput Phys 22:403–434.

Goff SA, Goldberg AL. 1985. Production of abnormal proteins in *E. coli* stimulates transcription of Ion and other heat shock genes. Cell 41: 587–595.

Good L, Nielsen PE. 1998. Antisense inhibition gene expression in bacteria by PNA targeted to mRNA. Nat Biotechnol 16:355–358.

Goss PJ, Peccoud J. 1998. Quantitative modeling of stochastic systems in molecular biology by using stochastic Petri nets. Proc Natl Acad Sci USA 95:6750–6755.

Goss PJ, Peccoud J. 1999. Analysis of the stabilizing effect of Rom on the genetic network controlling ColE1 plasmid replication. Pac Symp Biocomput 65–76.

Gottesman S. 1989. Genetics of proteolysis in *Escherichia coli.* Ann Rev Genet 23:163–198.

Gottesman S, Maurizi MR. 1992. Regulation by proteolysis: Energy-dependent proteases and their targets. Microbiol Rev 56:592–621.

Harcum SW, Bentley WE. 1993. Response dynamics of 26, 34, 39, 54, and 80 kDa proteases in induced cultures of recombinant *Escherichia coli.* Biotechnol Bioeng 42:675–685.

Hendrick JP, Hartl FU. 1993. Molecular chaperone functions of heat-shock proteins. Annu Rev Biochem 62:349–384.

Herman C, Thevenet D, D'Ari R, Bouloc P. 1995. Degradation of sigma

32, the heat shock regulator in *Escherichia coli*, is governed by HflB. Proc Natl Acad Sci. USA 92:3516–3520.

Houry WA, Frishman D, Eckerskorn C, Lottspeich F, Hartl FU. 1999. Identification of in vivo substrates of the chaperonin GroEL. Nature 402:147–154.

Imanaka T, Aiba S. 1981. A perspective on the application of genetic engineering: Stability of recombinant proteins. Ann NY Acad Sci 369: 1–14.

Jubete Y, Maurizi MR, Gottesman S. 1996. Role of the heat shock protein DnaJ in the Lon-dependent degradation of naturally unstable proteins. J Biol Chem 217:30798–30803.

Jurgen B, Lin HY, Riemschneider S, Scharf C, Neubauer P, Schmid R, Hecker M, Schweder T. 2000. Monitoring of genes that respond to overproduction of an insoluble recombinant protein in *Escherichia coli* glucose-limited fed-batch fermentations. Biotechnol Bioeng 70: 217–224.

Kanemori M, Mori H, Yura T. 1994. Induction of heat shock proteins by abnormal proteins results from stabilization and not increased synthesis of σ^{32} in *Escherichia coli.* J Bacteriol 176:5648–5653.

Kitagawa M, Wada C, Yoshioka S, Yura T. 1991. Expression of ClpB, an analog of the ATP-dependent protease regulatory subunit in *Escherichia coli,* is controlled by a heat shock sigma factor (sigma 32). J Bacteriol 173:4247–4253.

Kurtz TG. 1972. The Relationship between stochastic and deterministic models for chemical reactions. J Chem Phys 57:2976–2978.

Lesley SA, Thompson NE, Burgess RR. 1987. Studies of the role of the *Escherichia coli* heat shock regulatory protein σ^{32} by the use of monoclonal antibodies. J Biol Chem 262:5404–5407.

Marsan MA, Balbo G, Conte G, Donatelli S, Franceschinis G. 1995. Modelling with generalized stochastic petri nets. Chichester, UK: John Wiley & Sons.

McAdams HH, Arkin A. 1997. Stochastic mechanisms in gene expression. Proc Natl Acad Sci USA 94:814–819.

McAdams HH, Arkin A. 1998. Simulation of prokaryotic genetic circuits. Annu Rev Biophys Biomol Struct 27:199–224.

McAdams HH, Arkin A. 1999. It's a noisy business! Genetic regulation at the nanomolar scale. Trends Genet 15:65–69.

Mogk A, Tomoyasu T, Goloubinoff P, Rudiger S, Roder D, Langen H, Bukau B. 1999. Identification of thermolabile *Escherichia coli* proteins: Prevention and reversion of aggregation by DnaK and ClpB. EMBO J 18:6934–6949.

Muffler A, Barth M, Marschall C, Hengge-Aronis R. 1997. Heat shock regulation of σ^{s} turnover: A role for DnaK and relationship between stress responses mediated by σ^{s} and σ^{32} *Escherichia coli.* J Bacteriol 179:445–452.

Murray JAH, editor. 1992. Antisense RNA and DNA. New York: Wiley-Liss.

Nagai H, Yuzawa H, Yura T. 1991. Interplay of two cis-acting mRNA regions in translational control of sigma 32 synthesis during the heat shock response of *Escherichia coli.* Proc Natl Acad Sci USA 88: 10515–10519.

Neidhardt FC, Curtis R III, Ingraham JL, Lin ECC, Low KB, Magansik B, Reznikoff WS, Riley M, Schaechter M, Umberger HE, editors. 1996. *Escherichia coli* and *Salmonella:* Cellular and molecular biology. Washington, DC: ASM.

Neidhardt FC, VanBogelen RA. 1981. Positive regulatory gene for temperature-controlled proteins in *Escherichia coli.* Biochem Biophys Res Commun 100:894–900.

Ouchi Y, Tazaki E. 1998. Medical diagnostic system using fuzzy coloured Petri nets under uncertainty. Medinfo 9:675–679.

Parsell DA, Lindquist S. 1993. The function of heat-shock proteins in stress tolerance: Degradation and reactivation of damage proteins. Ann Rev Genetics 27:437–496.

Ramirez DM, Bentley WE. 1995. Fed-batch feeding and induction policies that improve foreign protein synthesis and stability by avoiding stress response. Biotechnol Bioeng 47:596–608.

Ramirez DM, Bentley WE. 1999. Characterization of stress and protein turnover from protein overexpression in fed-batch *E. coli* cultures. J Biotechnol 71:39–58.

Reddy VN, Mavrovouniotis ML, Liebman MN. 1993. In: Hunter L, et al., eds. Proceedings First International Conference on Intelligent Systems for Molecular Biology. AAAI Press: Menlo Park, CA. Petri net representations in metabolic pathways. ISMB 1:328–36.

Sanders WH. 1995. UltraSAN user's manual. Version 3.0. Urbana-Champaign, IL: Center for Reliable and High-Performance Computing, University of Illinois.

Srivastava R, Cha HJ, Peterson MS, Bentley WE. 2000. Antisense down-regulation of sigma(32) as a transient metabolic controller in *Escherichia coli:* Effects on yield of active organophosphorus hydrolase. Appl Environ Microbiol 66:4366–4371.

Strauss DB, Walter WA, Gross CA. 1987. The heat shock response of *E. coli* is regulated by changes in the concentration of σ^{32}. Nature 329: 348–391.

Strauss DB, Walter WA, Gross CA. 1989. The activity of σ^{32} is reduced under conditions of excess heat shock protein production in *Escherichia coli.* Genes Devel 3:2003–2010.

Strauss DB, Walter WA, Gross CA. 1990. DnaK, DnaJ, and GrpE heat shock proteins negatively regulate heat shock gene expression by controlling the synthesis and stability of σ^{32}. Genes Devel 4:2202–2209.

Tatsuta T, Tomoyasu T, Bukau B, Kitagawa M, Mori H, Karata K, Ogura T. 1998. Heat shock regulation in the ftsH null mutant of *Escherichia coli:* Dissection of stability and activity control mechanisms of sigma32 in vivo. Mol Microbiol 30:583–593.

Tilly K, Spence J, Georgopoulos C. 1989. Modulation of the stability of *Escherichia coli* heat shock regulatory factor σ^{32}. J Bacteriol 171: 1585–1589.

Tomoyasu T, Gamer J, Bukau B, Kanemori M, Mori H, Ritman AJ, Oppenheim AB, Yura T, Yamanaka K, Niki H, Hiraa S, Ogura T. 1995. *Escherichia coli* FtsH is a membrane-bound, ATP-dependent protease which degrades the heat-shock transcription factor σ^{32}. EMBO J 14: 2551–2560.

Tomoyasu T, Ogura T, Tatsuta T, Bukau B. 1998. Levels of DnaK and DnaJ provide tight control of heat shock gene expression and protein repair in *Escherichia coli.* Mol Microbiol 30:567–581.

Yura T, Nagai H, Mori H. 1993. Regulation of the heat-shock response in bacteria. Annu Rev Microbiol 47:321–350.